Chapter 1

Yolk Dynamics in Amphibian Embryos

Problem presented by: Richard Gordon (Department of Radiology, University of Manitoba)

Participants: C. Sean Bohun (Department of Science, University of Ontario Institute of Technology), Chris Breward (Mathematical Institute, University of Oxford), Ellis Cumberbatch (School of Mathematical Sciences, Claremont Graduate University), George Djoumna (Département de mathématics et de statistique, Université Laval), Ahmed ElSheikh (Department of Civil Engineering, McMaster University), JF Williams (Department of Mathematics, Simon Fraser University), Jonathan Wylie (Department of Mathematics, City University of Hong Kong)

Report prepared by: C. Sean Bohun[1] and Chris Breward[2].

1.1 Introduction

This problem was proposed by the Manitoba Institute of Child Health and investigated at the First Fields-MITACS Industrial Problem-Solving Workshop. The impetus for this work is to attempt to understand the role that gravity plays in the development of embryos. One of the most serious obstacles that the group found in this field is the lack of a complete set of physical parameters for any given embryo. Consequently, it was decided early on that no time would be spent modelling behaviour for which there was no experimental evidence.

Three processes observed in development of the egg prior to the first cell division were investigated. These include:

- the up-righting phase (first minute),
- the delay until cortical rotation initiates (up to one hour),
- the cortical rotation (~ 30 minutes).

The hope was that in understanding these simple processes, one would be able to understand some of the interesting behaviour of the egg described in Section 1.1.3 when it is rotated manually.

[1] sean.bohun@uoit.ca

[2] breward@maths.ox.ac.uk

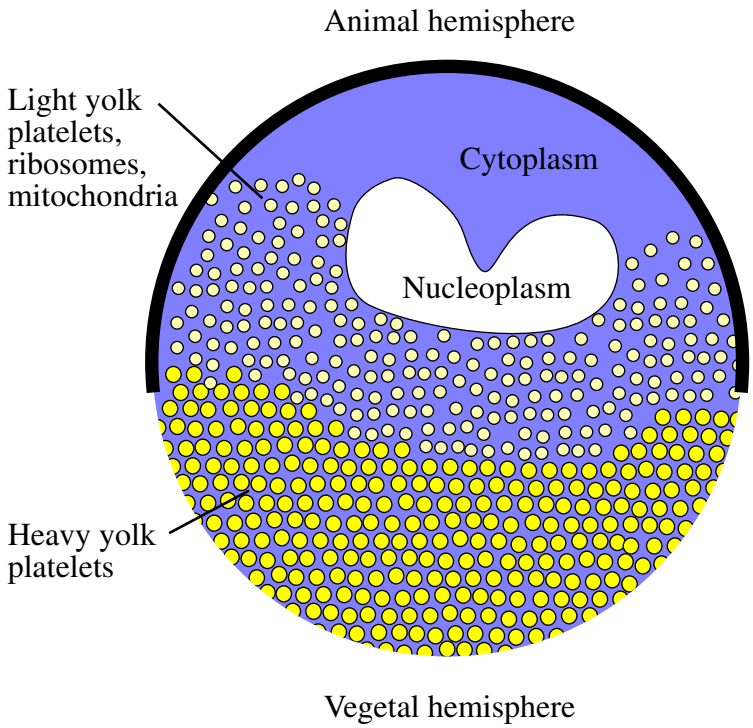

Figure 1.1: Structure of a mature oocyte.

1.1.1 Structure of the egg

Figure 1.1 illustrates a mature amphibian oocyt (unfertilized egg) and its internal structure. Contained within the oocyte is a nucleus containing nucleoplasm, and suspended in viscous cytoplasm are yolk platelets, ribosomes, and mitochondria. The yolk platelets store lipoproteins that are packed into a regular array and provide energy for the developing cell. They vary in size and density with an average diameter of $12\,\mu$m [23] for those platelets located in the vegetal hemisphere.

The periphery of the cell is quite complicated consisting of a series of interconnected layers. Outermost is a monolayer of follicle cells which are bound to the follicular epithelium that encases the oocyte. Beneath the follicular epithelium is the vitelline envelope which is roughly $1-2\,\mu$m in thickness and consists of a network of fibres that range in diameter from $40-70\,$nm. Within $200\,$nm of the surface of the plasma membrane are the cortical and pigment granules. Stereo micrographs of these structures can be found in [8]. The animal hemisphere is characterized by many pigment granules and cortical granules of $1.5\,\mu$m in diameter whereas the vegetal hemisphere has significantly less pigment granules and cortical granules of $2.5\,\mu$m in diameter [5]. A detailed view of the cell periphery can be found in [16] or in [5] and the references cited therein.

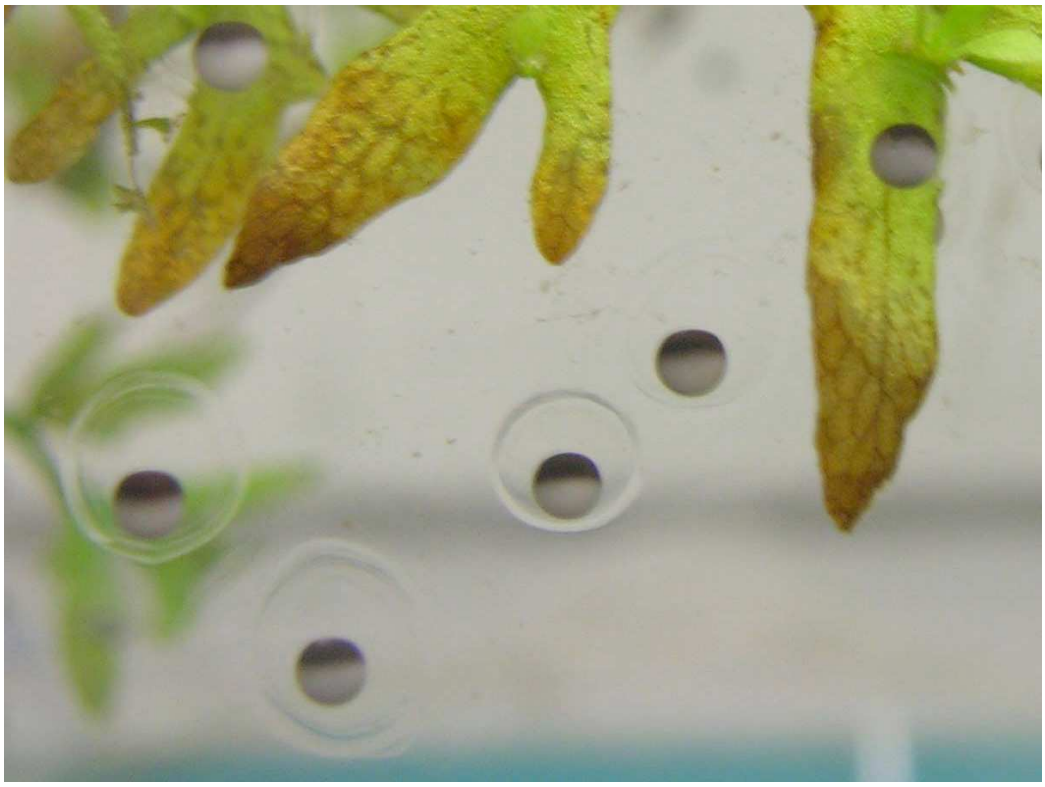

Figure 1.2: Typical axolotl eggs and their encapsulating gel after the up-righting phase (Courtesy of Susan Crawford-Young).

1.1.2 Egg activation

Fertilized eggs are released from the female in random orientations which persist even though they were activated through fertilization before release. In urodele amphibians such as the axolotl, many sperm enter the egg, but only one sperm nucleus fuses with the egg nucleus. When a fertilizing sperm penetrates the plasma membrane, the cortical granules break down and release their contents to the surface of the egg. Swelling on contact with water, the contents of the granules expand the space that lies between the plasma membrane and the vitelline envelope forming the perivitelline space [9]. At the same time the vitelline envelope hardens and prevents any further penetration by sperm. Once the perivitelline space has formed and the animal hemisphere contracts, the egg is freed of its connections to its surrounding membranes permitting the reorientation of the eggs via gravity. Average rates of rotation are typically 0.26 rpm [9] and the up-righting itself is hypothesized to be a result of the different yolk densities. Figure 1.2 shows axolotl eggs after up-righting. They appear to be axially symmetric, though inversion experiments [13, 21, 22] suggest that this may only apply to the cortex (cell membrane and underlying attached cytoplasm), i.e., developmentally the embryo may be spherically symmetric at this stage.

Further asymmetry within the egg is introduced by a reorganization of the cytoplasm at about the halfway point between the moment of fertilization and time of first cell division. The

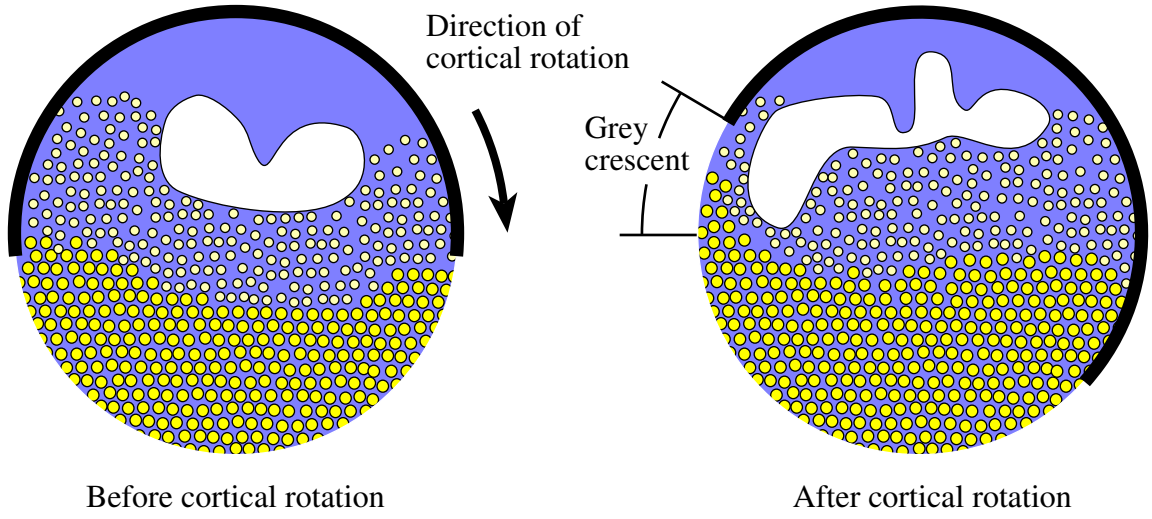

Figure 1.3: Eggs before and after cortical rotation.

reorganization occurs with a 30° rotation[3] of the cortex relative to the rest of the cell body [9] and is depicted in Figure 1.3. The portion of the egg exposed by moving the animal hemisphere becomes covered with the clear vegetal hemisphere and as a result forms a grey crescent. This region of the egg becomes the dorsal (back) side of the embryo and the opposite side of the egg forms the ventral (belly) side of the embryo. The grey crescent is only visible in certain amphibian eggs but many different techniques have been developed to visualize the subcortical rotation in many species.

1.1.3 The role of gravity

Gravity does seem to play a role in the development of the embryo but its effect is paradoxical. This was demonstrated in a sequence of experiments where the egg was immobilized and rotated manually. Four situations were examined with an initially inverted egg.

1. An initial rotation of $15° - 90°$ for 30 minutes and then manually up-righting the egg causes the dorsal lip of the embryo to reposition to the side of the egg opposing gravity but otherwise produces normal offspring [3].

2. Eggs irradiated with ultraviolet light typically create offspring with morphological defects. These defects can be corrected with a manual rotation of the egg for 30 minutes [3].

3. A sustained rotation of 165° (nearly inverted) produces offspring that have an altered pigmentation. Sterility is enhanced for those eggs with a lower viscosity [21].

4. A sustained inversion at 180° creates eggs that divide normally but fail to produce offspring [22].

[3]Vincent [20] indicates rotations of $20° - 38°$ with an average of 28°. Maximum linear displacement is 300 μm at rates up to 10 μm/minute.

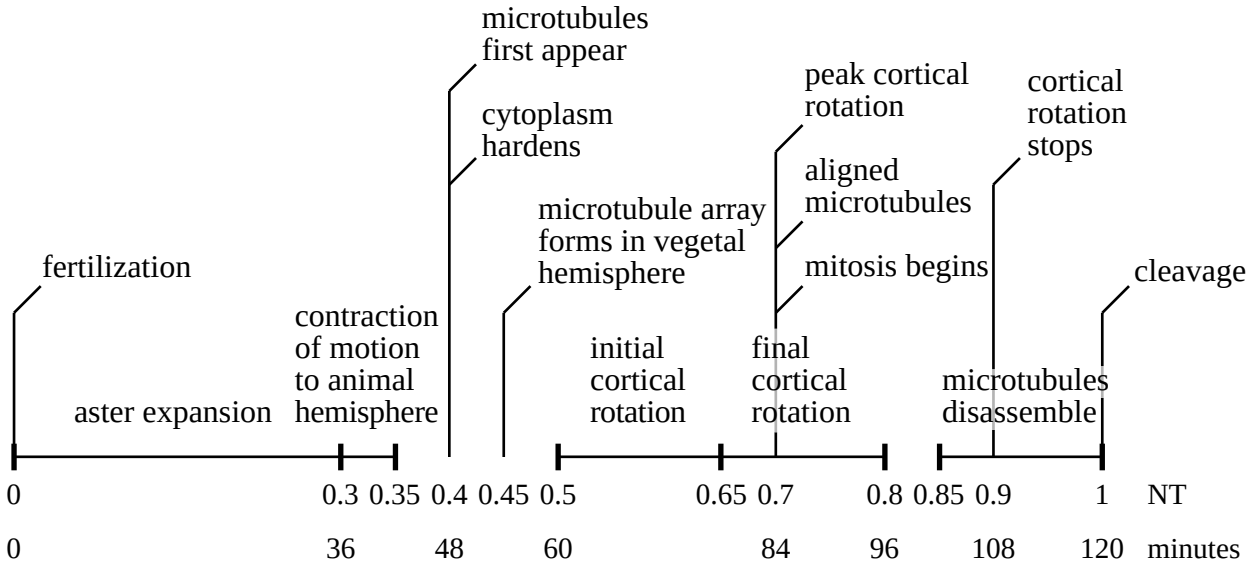

Figure 1.4: A timeline of significant events in the oocyte from fertilization to first cleavage.

A centrifuge has also been shown to be effective at orientating the cytoplasm, provided the procedure starts before the initiation of cortical rotation. Conjoined twin tadpoles were formed by first irradiating the egg with ultraviolet light, centrifuging at $30g$ for 4 minutes at a 90° inclination and then centrifuged at $10g$ for 4 minutes at a 0° inclination. These offspring were characterized as doubly rescued from the irradiation [1]. Despite the strength of the acceleration in this latter case the eggs produce viable offspring.

1.1.4 Overall timeline

Each of the processes discussed above occurs at a specific time within the first cell cycle. Figure 1.4 depicts the various events and is an accumulation of data from several sources [1, 9, 10, 11, 20, 24]. The time units are labelled in both normalized time (NT) and in minutes. A time of 0 NT corresponds to the moment of fertilization and 1 NT is the time when the egg divides for the first time. There is some ambiguity in the literature with respect to the absolute time scale since 1 NT can take anywhere from $85 - 120$ minutes depending on the temperature [1]. For the remainder of this report we have assumed the upper bound of 1 NT = 120 minutes.

1.1.5 Physical data

We end this section with a summary of the geometry and physical constants that were inferred from the embryological literature. Reported sizes of yolk platlets range from $2 - 14\,\mu$m in diameter, Neff et al. [14] identified three categories (small, medium and large) with densities of 1208, 1240, and 1290 kg/m^3 respectively. Wall et al. [23] specifies two sizes at different concentrations with a preponderance of the platelets about $12\,\mu$m in diameter. Light yolk platelets were found to have a density of 1210 kg/m^3 in concentrations of 7 g/ml whereas heavy

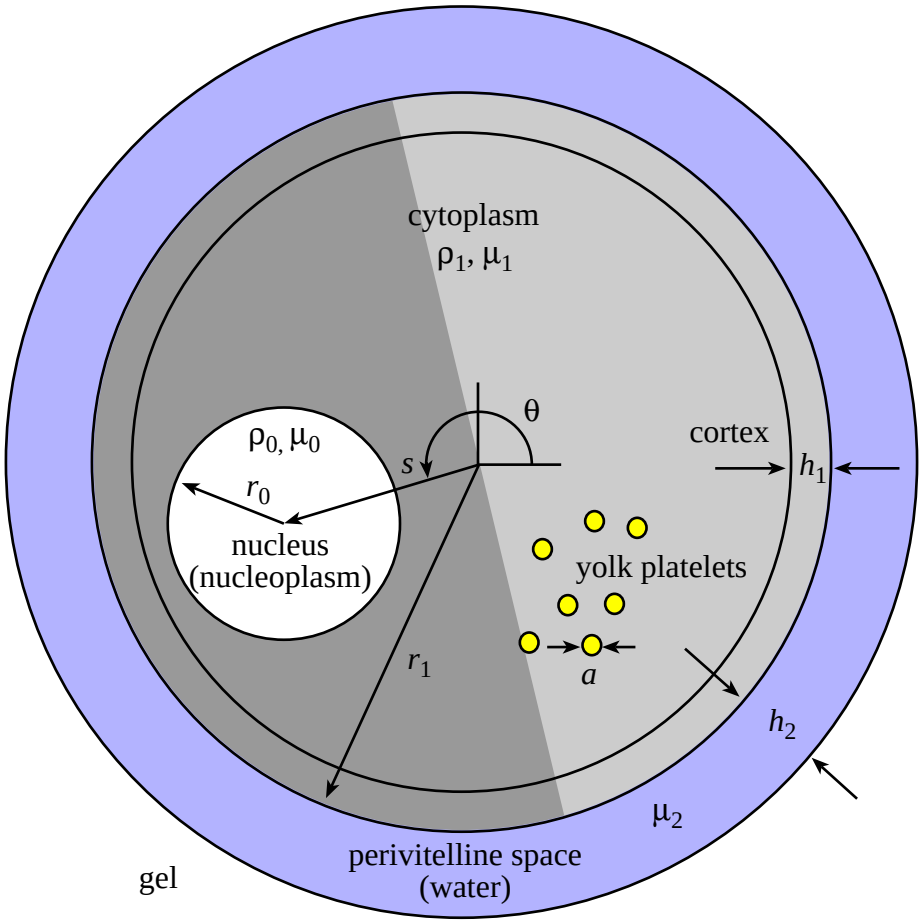

Figure 1.5: An idealized amphibian egg and its physical parameters.

platelets are more dense and occur in higher concentrations: $1230\,\mathrm{kg/m^3}$ at $40\,\mathrm{g/ml}$. Values used in the remainder of this report as well as a characteristic viscosity for the various regions of the egg are listed in Table 1.1. Most of the data is taken from the African clawed frog (*Xenopus laevis*) species.

Figure 1.5 illustrates the overall geometry of an amphibian egg showing the various regions of interest. The pigmentation variation seen in the previous images is represented by the dark and light grey shaded regions.

1.2 Up-righting phase

As previously described, once the eggs are released from the female and fertilized (or reverse, for urodele amphibians), the contents of the cortical granules are released into the gap between the plasma membrane and the vitelline membrane. Upon hydration this gap expands to form the perivitelline space, freeing the egg and causing it to rotate with the dark pigmentation area towards the top. Some of the characteristics of this up-righting motion are that it takes about

a minute to complete [9] and appears to be overdamped [6].

If the interior of the cell is sufficiently viscous then the up-righting can be approximated with a rigid body rotation. As discussed earlier, two of the main components of the interior of the egg are yolk platelets and cytoplasm. The platelets are membrane-bound spheres containing high concentrations of yolk protein so that interior can be thought of as a colloidal suspension. To determine how long it would take a yolk platelet of diameter a to traverse the length of the egg we apply Stokes' law to find the terminal velocity

$$v_\infty = \frac{1}{18}\frac{(\rho_2 - \rho_1)ga^2}{\mu_1} = 3.92 \times 10^{-7} \text{ m/s}$$

using the data in Table 1.1. This implies that it would take 5.1×10^3 seconds for the platelet to fall the 2 mm length of the egg. Since the up-righting occurs on the time scale of a minute, during this phase the interior of the egg can be approximated as solid.

Referring back to Figure 1.5, the nucleus is set inside a cell body and has three forces acting on it. The gravitational force acts through its centre of mass. Buoyancy acts through the centre of buoyancy which is simply the centre of mass of the displaced fluid. Finally, the viscous drag force opposes the motion in the fluid bearing region of the perivitelline space. Denoting θ as the angular displacement of the nucleus and I_0 as the moment of inertia of the cell,

$$I_0\ddot{\theta} = \tau_{\text{buoy}} + \tau_{\text{gravity}} + \tau_{\text{drag}}, \qquad \theta(0) = \theta_0, \quad \dot{\theta}(0) = 0. \tag{1.1}$$

Using the values in Table 1.1 we find that

$$I_0 \lesssim \frac{2}{5}m_1 r_1^2 = \frac{8}{15}\pi\rho_1 r_1^5 \simeq 2.8 \times 10^{-11}, \tag{1.2}$$

Table 1.1: Physical properties of a typical amphibian egg.

Density (kg/m^3)		
Nucleoplasm	$\rho_0 = 1000$	
Cytoplasm	$\rho_1 = 1100$	
Yolk platelets	$\rho_2 = 1200$	[14]
Dynamic Viscosity (kg/m/s)		
Nucleoplasm	$\mu_0 = 5 \times 10^{-3}$	[12]
Cytoplasm	$\mu_1 = 20 \times 10^{-3}$	[18]
Water	$\mu_2 = 1 \times 10^{-3}$	
Lengths (m)		
Nucleus diameter	$2r_0 = 7 \times 10^{-4}$	
Egg diameter	$2r_1 = 2 \times 10^{-3}$	[14]
Yolk platelet diameter	$a = 12 \times 10^{-6}$	[14]
Nucleus displacement	$s = 7 \times 10^{-4}$	
Cortex width	$h_1 = 20 \times 10^{-6}$	[16]
Perivitelline space	$h_2 = 3 \times 10^{-6}$	[25]

and

$$\tau_{\text{buoy}} + \tau_{\text{gravity}} = \frac{4}{3}\pi r_0^3(\rho_1 - \rho_0)gs\cos\theta \simeq 3.7 \times 10^{-10}\cos\theta, \tag{1.3}$$

where I_0 neglects the effect of the lower density region occupied by the nucleus. For the drag we need to take into account the variation in speed over the surface of the sphere. At an azimuthal angle of φ, the infinitesimal torque is

$$d\tau_{\text{drag}} = -\mu_2(r_1\sin\varphi)\dot{\theta}\left(\frac{r_1\sin\varphi}{h_2}\right)\,dA = -2\pi r_1^4\frac{\mu_2\dot{\theta}}{h_2}\sin^3\varphi\,d\varphi.$$

Integration over $0 \le \varphi \le \pi$ gives the expression

$$\tau_{\text{drag}} = -\frac{4}{3}\pi r_1^4\frac{\mu_2\dot{\theta}}{h_2} \sim -1.4 \times 10^{-9}\dot{\theta}. \tag{1.4}$$

Due to their relative smallness, the inertial terms do not contribute significantly to the motion. Neglecting them reduces (1.1)-(1.4) to the simplified expression

$$\dot{\theta} \simeq \frac{sr_0^3}{r_1^4}\frac{h_2 g(\rho_1 - \rho_0)}{\mu_2}\cos\theta, \qquad \theta(0) = \theta_0, \quad \dot{\theta}(0) = 0 \tag{1.5}$$

with solution curves illustrated in Figure 1.6. Notice that the time to up-right is typically less than a minute and the behaviour is essentially exponential. Using reported rotational speeds of anywhere from 0.026 to 0.54 rpm [9] and the fact that the maximal rate of rotation occurs when $\theta = 0$ we can determine the size of the perivitelline space as

$$\frac{0.026(2\pi)}{60}\,\frac{r_1^4\mu_2}{sr_0^3 g(\rho_1 - \rho_0)} \le h_2 \le \frac{0.54(2\pi)}{60}\,\frac{r_1^4\mu_2}{sr_0^3 g(\rho_1 - \rho_0)}$$

or $0.092\,\mu\text{m} \le h_2 \le 1.9\,\mu\text{m}$. These values are quite possible since this space is created by the swelling contents of corticle granules that are themselves typically only $1.5\,\mu$m in diameter.

1.3 Delay until cortical rotation

Once the egg has up-righted, the yolk platelets in the cytoplasm will settle out until they reach an equilibrium distribution. To study this behaviour we approximate the interior of the egg with a one-dimensional two phase flow model (see [7]) for the yolk/cytoplasm colloid as illustrated in Figure 1.7[4]. In what follows α and β are the volume fractions of the yolk and cytoplasm which move with speeds u_α and u_β respectively. Conservation of mass for each phase can then be written as

$$\alpha_t + (\alpha u_\alpha)_y = 0, \qquad \beta_t + (\beta u_\beta)_y = 0. \tag{1.6}$$

Assuming that space is completely filled by yolk and cytoplasm, we write

$$\alpha + \beta = 1, \tag{1.7}$$

[4]We neglect the presence of the nucleus in this section.

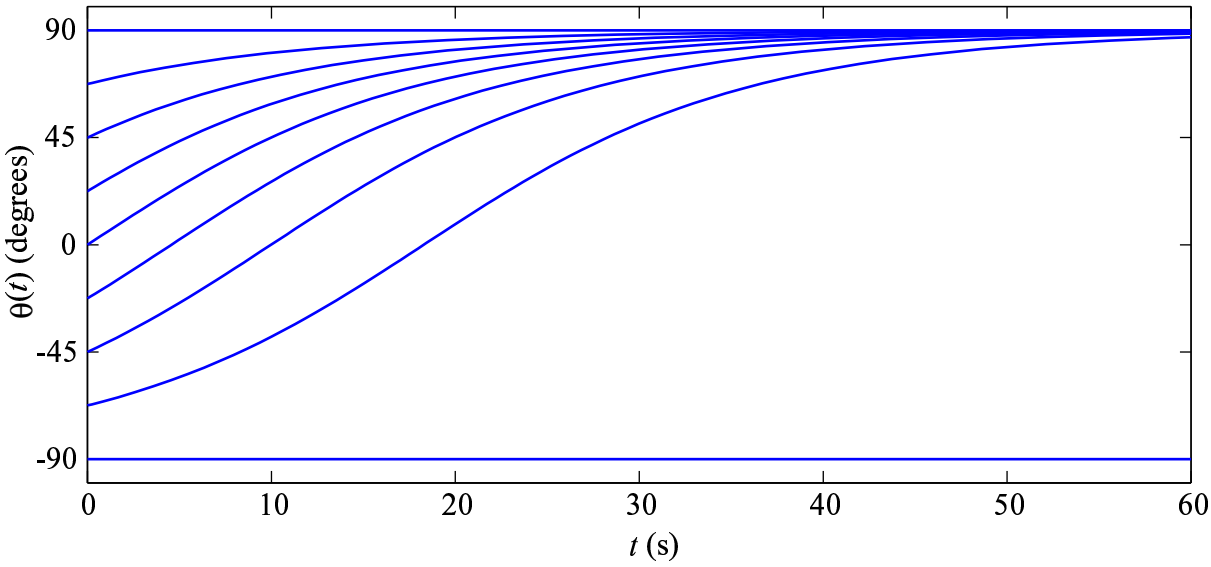

Figure 1.6: Solution curves to (1.5) with various initial values $-\pi/2 \leq \theta_0 \leq \pi/2$.

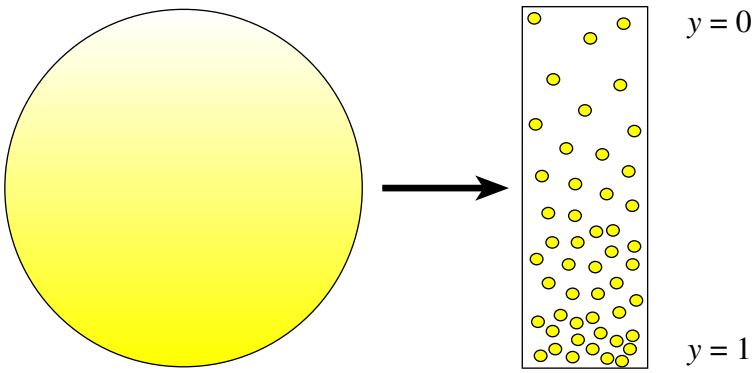

Figure 1.7: One-dimensional approximation of the interior of the egg.

which is known as the no-voids condition. Neglecting inertia and introducing p_α and p_β for the averaged isotropic pressure in each phase, μ_α and μ_β for the viscosity of each phase, g as the acceleration due to gravity, and τ_α and τ_β for the deviatoric stresses, conservation of momentum for each phase leads us to

$$(-\alpha p_\alpha + \alpha\tau_\alpha)_y + (p_\alpha - \tau_{\alpha i})\alpha_y - \frac{\mu_\alpha}{a^2}\alpha f(\alpha)(u_\alpha - u_\beta) + \rho_\alpha g\alpha = 0, \tag{1.8}$$

$$(-\beta p_\beta + \beta\tau_\beta)_y + (p_\beta - \tau_{\beta i})\beta_y + \frac{\mu_\alpha}{a^2}\alpha f(\alpha)(u_\alpha - u_\beta) + \rho_\beta g\beta = 0, \tag{1.9}$$

where $\tau_{\alpha i}$ and $\tau_{\beta i}$ are the stresses at the interfaces. The first two terms are the bulk-averaged and surface-averaged contributions to the stress from the phases themselves, the third term in these equations represents drag one phase on the other (modelled by f), and the final term represents

the gravitational force. Continuity of stress at the interface between yolk and cytoplasm gives

$$-p_\alpha + \tau_{\alpha i} - (-p_\beta + \tau_{\beta i}) = -\gamma\kappa, \tag{1.10}$$

where γ is the average interfacial tension and κ is the average interfacial curvature.

In order to close the model we have to pose four constitutive laws, describing the behaviour of the two fluids and what happens with the stress at the interface. Assuming both phases behave as viscous liquids, we write

$$\tau_\alpha = \mu_\alpha u_{\alpha y}, \qquad \tau_\beta = \mu_\beta u_{\beta_y}, \qquad \tau_{\alpha i} = -\mu_\alpha f_1(\alpha) u_{\alpha y}, \qquad \tau_{\beta i} = -\mu_\beta f_2(\beta) u_{\beta_y},$$

where f_1 and f_2 are functions associated with the geometry of the system and the ease of motion of the liquids.

It is straightforward to reduce these ten expressions to three. We nondimensionalise the resulting equations using

$$y = L\hat{y}, \qquad u = U\hat{u} = \frac{\rho_\alpha g a^2}{\mu_\alpha}\hat{u}, \qquad t = \frac{L\mu_\alpha}{\rho_\alpha g a^2}\hat{t}, \qquad p = \frac{\mu_\alpha U L}{a^2}\hat{p}, \qquad \epsilon = \frac{a}{L},$$

to yield, dropping hats,

$$\alpha_t + (\alpha u)_y = 0, \tag{1.11}$$

$$\alpha p_y = \alpha\left(1 - \frac{fu}{1-\alpha}\right) + \epsilon^2\left((\alpha u_y)_y + f_1\alpha_y u_y\right), \tag{1.12}$$

$$p_y = \bar{\rho} + (1-\bar{\rho})\alpha + \epsilon^2\left((\alpha u_y)_y + f_1\alpha_y u_y - (1-\alpha)(f_1 u_y)_y + \Gamma\right) \tag{1.13}$$

where $\bar{\rho} = \rho_\beta/\rho_\alpha$, and

$$\Gamma = -\frac{\mu_\beta}{\mu_\alpha}\left[\left((1-\alpha)\left(\frac{\alpha u}{1-\alpha}\right)_y\right)_y - f_2\alpha_y\left(\frac{\alpha u}{1-\alpha}\right)_y + (1-\alpha)\left(f_2\left(\frac{\alpha u}{1-\alpha}\right)_y\right)_y\right]. \tag{1.14}$$

To leading order in ϵ, we find that

$$\alpha_t + (\alpha u)_y = 0, \qquad u = (1-p_y)\frac{1-\alpha}{f}, \qquad p_y = \bar{\rho} + (1-\bar{\rho})\alpha,$$

in otherwords,

$$\alpha_t + \left(\frac{(1-\bar{\rho})\alpha(1-\alpha)^2}{f}\right)_y = 0. \tag{1.15}$$

We suppose that we know the initial distribution of the yolk platelets, so that we write

$$\alpha(y,0) = \alpha_0(y). \tag{1.16}$$

At the top and bottom of the egg, we suppose that there is no motion of either phase (that is, since the fluids are viscous we impose the no slip condition) and so we set $u = 0$. This is

not possible at both the top and bottom surfaces as seen by the leading-order outer solution, so the viscous stresses that we have neglected to leading order become important. Scaling into the boundary layers at the top and bottom of the egg, we find that conservation of mass leads to the condition

$$u\alpha = 0$$

at $y = 0$ and $y = 1$. We pick $u = 0$ throughout the bottom boundary layer (with consequence that $\alpha = 1$ at $y = 1$). In the top boundary layer, we choose $\alpha = 0$. We now consider the evolution of three relevant initial conditions (a) a linear yolk gradient, (b) an inverted egg (with a linear gradient) and (c) a well-mixed egg. We set $f = 1$ for simplicity, since we are unsure of the actual functional form, and we scale $t = \tau/(1-\rho)$ to remove the explicit dependence on ρ. The timescale, T, for the drainage problem is therefore given by

$$T = \frac{L\mu_\alpha}{(\rho_\alpha - \rho_\beta)ga^2} \sim 700\,\mathrm{s}, \tag{1.17}$$

using the values given in Table 1.1.

Our problem is then to solve

$$\alpha_\tau + \left(\alpha(1-\alpha)^2\right)_y = 0, \qquad y \in (0,1),\ \tau > 0, \tag{1.18}$$

with an initial condition appropriate to each case and keeping in mind the boundary conditions discussed in the previous paragraph.

1.3.1 Settling of yolk from a linear gradient

We suppose that

$$\alpha(y,0) = y, \tag{1.19}$$

and we note that the initial linear gradient satisfies the boundary conditions discussed in the previous section. We solve (1.18) and (1.19) using the method of characteristics, which, for $\tau < 1/4$, yields

$$\alpha(y,t) = \begin{cases} 0 & 0 \le y < \tau \\ \frac{1}{6}\left[4 - \frac{1}{\tau} + \sqrt{\left(4-\frac{1}{\tau}\right)^2 - 12\left(1-\frac{y}{\tau}\right)}\right], & \tau < y \le 1. \end{cases} \tag{1.20}$$

At $\tau = 1/4$ a shock forms and we use the Rankine-Hugoniot condition (see [15]) to find the position of the shock. Denoting the shock position by $y = s(\tau)$, we have

$$\frac{ds}{d\tau} = \frac{[\alpha(1-\alpha)^2]}{[\alpha]}, \tag{1.21}$$

where the square brackets denote the jump in the quantity inside the brackets as the shock is traversed. In this case, since the volume fraction of yolk platelets is zero above the shock, (1.21) becomes

$$\frac{ds}{d\tau} = (1-\alpha_+)^2, \tag{1.22}$$

where α_+ is the solution given in (1.20) and evaluated at $y = s$, i.e.

$$\alpha_+ = \frac{1}{6}\left[4 - \frac{1}{\tau} + \sqrt{\left(4 - \frac{1}{\tau}\right)^2 - 12\left(1 - \frac{s}{\tau}\right)}\right]. \tag{1.23}$$

The initial condition for the shock position is $s = 1/4$ at $\tau = 1/4$. We solve (1.22) numerically and show the position of the shock in (y, τ) space in the upper figure of Figure 1.8. As $\tau \to \infty$, $s \to 1/2$, and the liquid separates into cytoplasm at the top of the egg, and yolk at the bottom. We show the volume fraction of the yolk platelets as it evolves in the lower figure of Figure 1.8. We note that the yolk takes an infinite amount of time to reach its steady state and that the drainage is fastest at the start. Indeed after 15 minutes, the yolk platelets reside below $y = 0.45$ (i.e. within 10% of their final position).

1.3.2 Settling of an inverted egg

In this case, we set

$$\alpha(y, 0) = 1 - y. \tag{1.24}$$

We find that a shock immediately develops at the bottom of the egg, across which the yolk volume fraction jumps to unity. A second shock propagates in from the top of the egg, initiating at $\tau = 1/2$, across which the volume fraction jumps from zero. Denoting these two shocks as $s_{\text{top}}(\tau)$ and $s_{\text{bot}}(\tau)$ respectively, we find that the solution is

$$\alpha(y,t) = \begin{cases} 0 & 0 \le y \le s_{\text{top}}(\tau) \\ \frac{1}{6}\left[4 - \frac{1}{\tau} + \sqrt{\left(4 - \frac{1}{\tau}\right)^2 - 12\left(1 + \frac{1}{\tau} - \frac{y}{\tau}\right)}\right], & s_{\text{top}}(\tau) \le y \le s_{\text{bot}}(\tau), \\ 1 & s_{\text{bot}}(\tau) \le y \le 1. \end{cases} \tag{1.25}$$

where the position of the shocks can be found by solving

$$\frac{ds_{\text{top}}}{d\tau} = \left(1 - \alpha(s_{\text{top}}, \tau)\right)^2, \qquad s_{\text{top}}(1/4) = 0, \tag{1.26}$$

and

$$\frac{ds_{\text{bot}}}{d\tau} = -\frac{\alpha(s_{\text{bot}}, \tau)\left(1 - \alpha(s_{\text{bot}}, \tau)\right)^2}{1 - \alpha(s_{\text{bot}}, \tau)} \qquad s_{\text{bot}}(0) = 0. \tag{1.27}$$

These two shocks collide at $y = 1/2$, $\tau = 2.6$ and the solution becomes

$$\alpha(y,t) = \begin{cases} 0, & 0 \le y < 1/2 \\ 1, & 1/2 \le y \le 1, \end{cases} \tag{1.28}$$

for subsequent times, since the new shock created when these two collide satisfies $ds_{\text{end}}/d\tau = 0$. We show the characteristic projections and the evolution of the yolk volume fraction in Figure 1.9. We note that, in this case, the yolk reaches its steady state after a finite time, which is equivalent to 30 minutes.

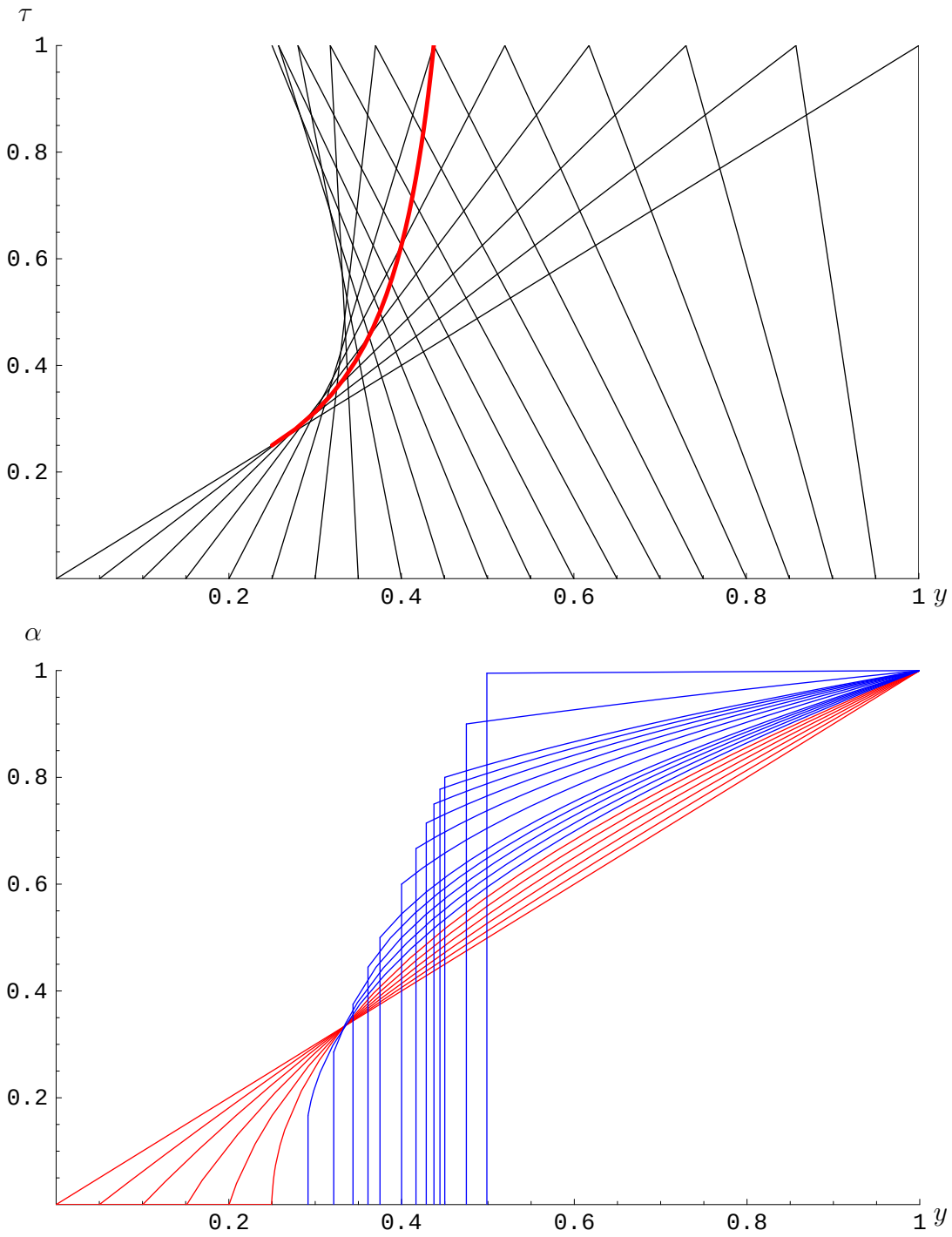

Figure 1.8: (upper) Characteristic projection in (y, τ) space. The red line shows the position of the shock. (lower) Graph showing the evolution of the yolk volume fraction. The red profiles are before the shock develops, the blue ones, afterwards.

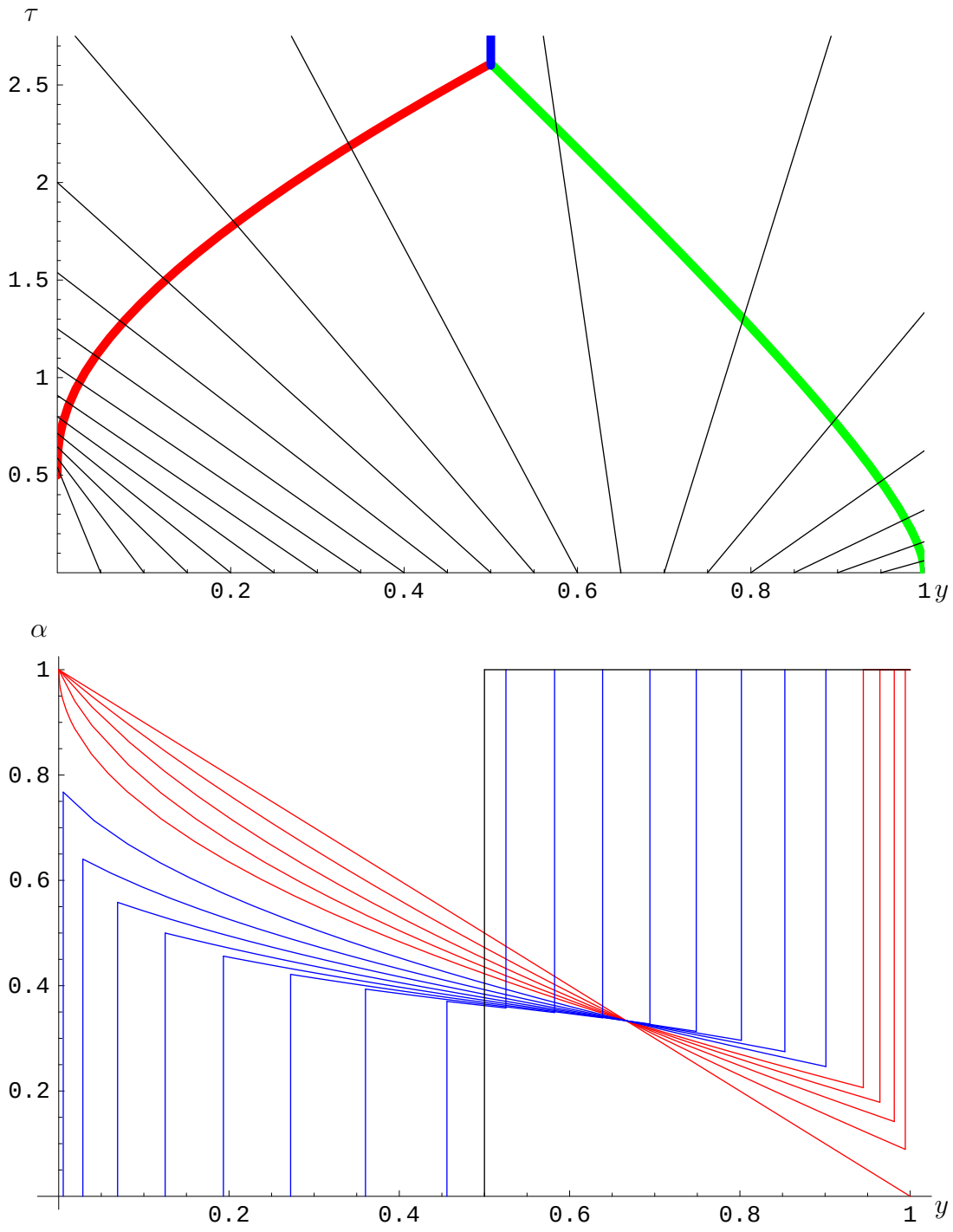

Figure 1.9: (upper) Characteristic projection in (y, τ) space. The red line shows the position of s_{top}, the green line shows the position of s_{bot} and the blue line shows the position of s_{end}. (lower) Graph showing the evolution of the yolk volume fraction. The red profiles are before the shock s_{top} develops, the blue ones, afterwards. The final state is shown in black.

1.3.3 Settling of a well-mixed egg

The final case we consider is the settling of an egg where the yolk is well mixed, so that the initial condition is

$$\alpha(y,0) = 1/2. \tag{1.29}$$

In this case, the solution is $\alpha = 1/2$ along parallel lines $\tau = 4(y_0 - y)$. However, the initial data cannot propagate into the triangle $1 - \tau/4 \le y \le 1$, and we introduce an expansion fan there (with α ranging from 1/2 to 1). Some of the characteristics in the fan intersect with those generated from the initial data so, as in the previous case, we have a shock propagating in from the base of the egg. The solution reads

$$\alpha(y,t) = \begin{cases} 0 & 0 \le y \le s_{\text{top}}(\tau) \\ 1/2 & s_{\text{top}}(\tau) \le y \le s_{\text{bot}}(\tau) \\ \frac{2+\sqrt{1-\frac{1-y}{\tau}}}{3}, & s_{\text{bot}}(\tau) \le y \le 1. \end{cases} \tag{1.30}$$

In this situation, it's easy to find $s_{\text{top}} = \tau/4$, and that s_{bot} satisfies

$$\frac{ds_{\text{bot}}}{dt} = \frac{\alpha^*(1-\alpha^*)^2 - \frac{1}{8}}{\alpha^* - \frac{1}{2}}, \qquad s_{\text{bot}}(0) = 1, \tag{1.31}$$

where

$$\alpha^* = \frac{2 + \sqrt{1 - \frac{1-s(\tau)}{\tau}}}{3}. \tag{1.32}$$

This solution holds until the two shocks collide, which occurs at τ^*, found by solving $s_{\text{top}}(\tau^*) = s_{\text{bot}}(\tau^*)$, and yielding $\tau = 1.788$, $y = 0.444$ and subsequently a final (slowly moving) shock propagates back down the egg allowing a relaxation to the steady state. The final shock initiates from $s_{\text{bot}}(\tau^*)$, and moves according to

$$\frac{ds_{\text{end}}}{dt} = (1-\alpha^*)^2, \qquad s_{\text{end}}(\tau^*) = s_{\text{bot}}(\tau^*). \tag{1.33}$$

We show the characteristic projection and the evolution of the yolk volume fraction in Figure 1.10, in which we can see that the yolk takes an infinite time to settle to the steady state. However, after 22 minutes, the yolk platelets are all below $y = 0.45$.

1.4 Cortical rotation

We now turn our attention to the rotation of the cortex that takes place typically around $t = 0.5$ in normalized time units or at about 60 minutes. Some recent developments [2, 10, 11, 24] have begun to identify components involved in the cortical rotation but there is still a poor understanding of the details of the actual mechanism. What is known with some certainty is that the motor molecules dynein and kinesin both play a role in the process. In addition, recent measurements [4] have determined that one motor molecule is capable of producing about 6.2×10^{-12} N of force.

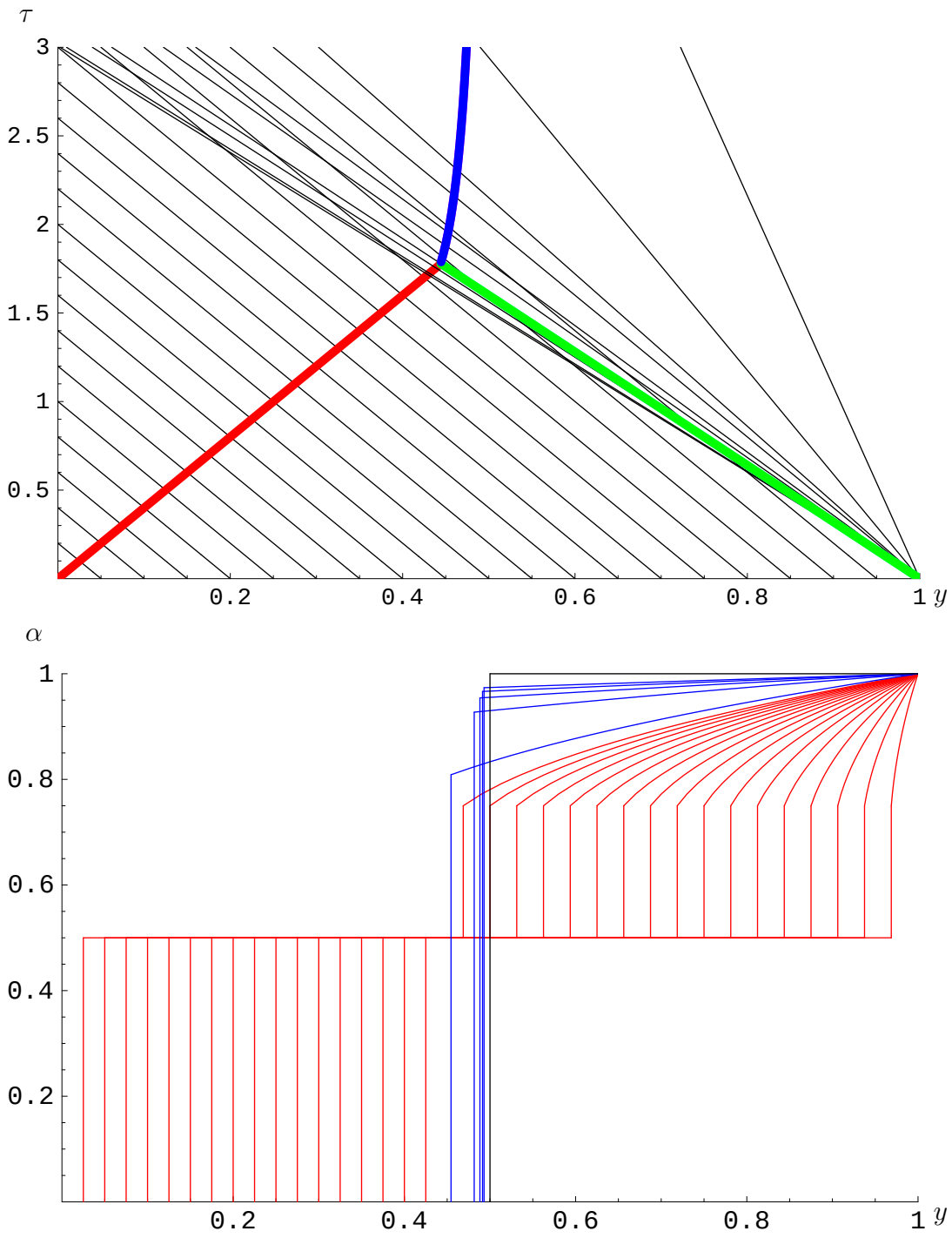

Figure 1.10: (upper) Characteristic projection in (y, τ) space. The red line shows the position of s_{top}, the green line shows the position of s_{bot} and the blue line shows the position of s_{end}. (lower) Graph showing the evolution of the yolk volume fraction. The red profiles are before the shock s_{end} develops, the blue ones, afterwards. The final state is shown in black.

Even though the electrokinetics of microtubules is still in its infancy [19], it is possible to determine the number of motor molecules that would be required to perform the cortical rotation. We know that the rotation rate is typically $\dot{\theta} = 30^{\circ}$ in 30 minutes $= \pi/180/60$ rad/s. As a result the linear speed at the surface of the egg ($r_1 = 1 \times 10^{-3}$ m) is $v_1 = r_1\dot{\theta}$ or $v_1 = 2.9 \times 10^{-7}$ m/s.

The drag force on the cortex is to a first approximation simply the surface area of the cortex multiplied by the viscous drag per unit area. Using the data in Table 1.1,

$$F_{\text{drag}} = 4\pi r_1^2 \mu_1 \left.\frac{\partial v}{\partial r}\right|_{r=r_1} = 4\pi r_1^2 \mu_1 \frac{v_1}{h_1} = 3.6 \times 10^{-9}\,\text{N}$$

indicating that about 590 of the roughly 10^4 available motor molecules would be required to achieve the observed rotation rate. Irrespective of the actual mechanism chosen there seems to be enough energy available to allow the rotation to occur.

There are two main difficulties that need to be overcome before any further modelling can commence. First, the generation of microtubules inside the egg and the motion of motor molecules along these microtubles could be modelled but as mentioned earlier, it is not clear in the literature as to the actual mechanism. The second problem to overcome is an understanding of the switching on and off for the cortical rotation. It seems that this is biological in nature and there does not seem to be an appropriate model for this process. It is possible that cortical rotation is merely stopped by cell division. Artificially induced rotation in sea urchin eggs continues indefinitely [17].

1.5 Conclusions and Future Work

In our analysis of the yolk dynamics of the egg prior to the first cell division, three sub-problems were investigated. The up-righting phase was modelled with a simple buoyancy argument for a low density nucleus trapped inside a viscous cytoplasm and predicts an up-righting behaviour consistent with observations.

Once the egg has up-righted, the yolk platelets in the cytoplasm will settle out until they reach an equilibrium distribution. We described the settling of yolk platelets through the cytoplasm using a two phase model. We reduced the model to the simplest form possible and solved the resulting model analytically in three cases: a linear initial gradient of yolk platelets, an inverted egg, and a well mixed egg. We found that the inverted egg settled in finite time, while the other cases settled in infinite time (with the evolution being 90% complete within 15 minutes and 22 minutes respectively). In all three cases, a region devoid of yolk platelets formed near the top of the egg, and we were able to track the point at which the volume fraction became non-zero.

In the case where one inverts the egg, the yolk platelets are stationary after 30 minutes, in contrast with the upright egg case, where there is *always* motion of the fluid in the egg, albeit slow. This might suggest that yolk *motion* is needed for correct development of embryos. However, further speculation about links between the yolk platelet evolution and the development of the embryo will require further experimentation.

With respect to cortical rotation, we verified that motor molecules with the egg will have sufficient energy to cause the cortical rotation. However, a clear mechanism for how the rotation takes place has not been identified.

Future work along these lines could involve further development of the two-phase model to allow the inclusion of the nucleus and/or utilization of the correct egg geometry. An important step in the verification and refinement of the models used in this preliminary work is the direct observation of yolk platelets during the critical moments between fertilization and the first cell division.

1.6 Acknowledgements

The authors would like to acknowledge the Fields Institute and MITACS for their sponsorship of the FMIPW event. We would also like to take this opportunity to thank Huaxiong Huang, Barbara Keyfitz and Nilima Nigam for organizing the event. Their hard work and dedication ensured the success of the workshop.

Bibliography

[1] Black, S.D. & Gerhart, J.C. (1986). High-Frequency Twinning of Xenopus laevis Embryos from Eggs Centrifuged before First Cleavage. *Developmental Biology*, **116**, 1, pp. 228-240.

[2] Brito, D.A. et al. (2005). Pushing Forces Drive the Comet-like Motility of Microtubule Arrays in Dictyostelium. *Molecular Biology of the Cell*, **16**, 7, 3334-3340.

[3] Chung, H. & Malacinski, G.M. (1980). Establishment of the Dorsal/Ventral Polarity of the Amphibian Embryo: Use of Ultraviolet Irradiation and Egg Rotation as Probes. *Developmental Biology*, **80**, 1, pp. 120-133.

[4] Fisher, M.E. & Kolomeisky, A.B. (1999). The force exerted by a molecular motor. *Proceedings of the National Academy of Sciences of the United States of America*, **96**, 12, pp. 6597-6602.

[5] Gentry, M. (2006). Ultrastructure of the coelemic oocyte of Xenopus laevis. `http://131.229.114.77/microscopy/student%20projects/MilliecentGentry.html`

[6] Personal communication with Richard Gordon.

[7] Howell, P.D. & Muldoon, M. (2003). Two-phase modelling of air bubbles in ice cream. *Proceedings of the 46th ESGI* `http://www.maths-in-industry.org/24/`

[8] Larabell, C.A. (1993). A New Technique for Isolation and Visualization of the Xenopus Egg Cortex Reveals a Complex Cytoskeleton. *Journal of Structural Biology*, **110**, 2, pp. 154-159.

[9] Malacinski, G.M. & Neff, A.W. (1989). The Amphibian Egg as a Model System for Analyzing Gravity Effects. *Advances in Space Research*, **9**, 11, pp. 169-176.

[10] Marrari, Y. et al. (2003). Analysis of microtubule movement on isolated Xenopus egg cortices provides evidence that the cortical rotation involves dynein as well as Kinesin Related Proteins and is regulated by local microtubule polymerisation. *Developmental Biology*, **257**, 1, pp. 55-70.

[11] Marrari, Y., Rouvière, C. & Houliston, E. (2004). Complementary roles for dynein and kinesins in the Xenopus egg cortical rotation. *Developmental Biology*, **271**, 1, pp. 38-48.

[12] Marshall, W.F. et al. (1997). Interphase chromosomes undergo constrained diffusional motion in living cells. *Current Biology*, **7**, 12, pp. 930-939.

[13] Neff, A.W., Wakahara, M., Jurand, A. & Malacinski, G.M. (1984). Experimental analyses of cytoplasmic rearrangements which follow fertilization and accompany symmetrization of inverted Xenopus eggs. *Journal of Embryology and Experimental Morphology*, **80**, pp. 197-224.

[14] Neff, A.W., Smith, R.C. & Malacinski, G.M. (1986). Amphibian Egg Cytoplasm Response to Altered g-Forces and Gravity Orientation. *Advances in Space Research*, **6**, 12, pp. 21-28.

[15] Ockenden J.R., Howison, S.D., Lacey, A.A. & Movchan, A. (1999). Applied Partial Differential Equations. Oxford University Press.

[16] Sardet, C. et al. (2002). Structure and Function of the Cell Cortex from Oogenesis through Fertilization. *Developmental Biology*, **241**, 1, pp. 1-23.

[17] Schroeder, T.E. & D.E. Battaglia (1985). "Spiral asters" and Cytoplasmic Rotation in Sea Urchin Eggs: Induction in Strongylocentrotus purpuratus Eggs by Elevated Temperature. *Journal of Cell Biology*, **100**, 4, pp. 1056-1062.

[18] Valentine, M.T. et al. (2005). Mechanical Properties of Xenopus Egg Cytoplasmic Extracts. *Biophysical Journal*, **88**, 1, pp. 680-689.

[19] van den Heuval, M.G.L., de Graaff, M.P. & Dekker, C. (2006). Molecular Sorting by Electrical Steering of Microtubules in Kinesin-Coated Channels. *Science*, **312**, 5775, 910-914.

[20] Vincent, J., Oster, G.F. & Gerhart, J.C. (1986). Kinematics of Gray Crescent Formation in Xenopus Eggs: The Displacement of Subcortical Cytoplasm Relative to the Egg Surface. *Developmental Biology*, **113**, 1, pp. 484-500.

[21] Wakahara, M., Neff, A.W. & Malacinski, G.M. (1984). Topology of the germ plasm and development of primordial germ cells in inverted amphibian eggs. *Differentiation*, **26**, 3, pp. 203-210.

[22] Wakahara, M., Neff, A.W. & Malacinski, G.M. (1985). Development of delayed gastrulae and permanent blastulae from inverted Xenopus laevis eggs. *Acta embryologiae et morphologiae experimentalis*, **6**, pp. 193-209.

[23] Wall, D.A. & Meleka, I. (1985). An Unusual Lysosome Compartment Involved in Vitellogenin Endocytosis by Xenopus Oocytes. *The Journal of Cell Biology*, **101**, 5, part 1, pp. 1651-1664.

[24] Weaver, C. & Kimelman, D. (2004). Move it or lose it: axis specification in Xenopus. *Development*, **131**, 15, pp. 3491-3499.

[25] Inferred from the data in [8] and [9].